MethyleneCycloPropene: Local Vision of the first 1 B 2 excited state

Julien Racine, Mohamed Abdelhak Touadjine, Ali Rahmouni, Stéphane Humbel

▶ **To cite this version:**

Julien Racine, Mohamed Abdelhak Touadjine, Ali Rahmouni, Stéphane Humbel. MethyleneCyclo-Propene: Local Vision of the first 1 B 2 excited state. Journal of Molecular Modeling, 2017, 1116, pp.184 - 189. 10.1007/s00894-016-3191-x . hal-01539634

HAL Id: hal-01539634
https://hal.science/hal-01539634v1

Submitted on 15 Jun 2017

HAL is a multi-disciplinary open access archive for the deposit and dissemination of scientific research documents, whether they are published or not. The documents may come from teaching and research institutions in France or abroad, or from public or private research centers.

L'archive ouverte pluridisciplinaire **HAL**, est destinée au dépôt et à la diffusion de documents scientifiques de niveau recherche, publiés ou non, émanant des établissements d'enseignement et de recherche français ou étrangers, des laboratoires publics ou privés.

MethyleneCycloPropene: Local Vision of the first $^1B_2$ excited state.

Julien Racine,[1] Mohamed Abdelhak Touadjine,[2] Ali Rahmouni,[2] Stéphane Humbel[1*]

[1] Aix Marseille Université, Centrale Marseille, CNRS, iSm2 UMR 7313, 13397, Marseille, France
[2] Université Tahar Moulay de Saida, Laboratoire de Modélisation et de Méthodes de Calcul, BP 138 cité ENNASR 20000, Saida, Algérie

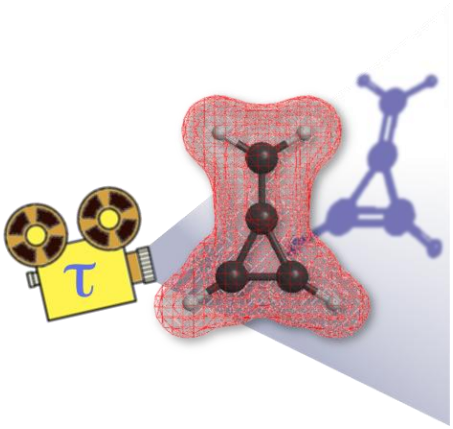

Graphical Abstract:

email : stephane.humbel@univ-amu.fr

Abstract

The $^1A_1$ ground and the first $^1B_2$ excited states of the methylenecyclopropene (triafulvene) are described by localized wave functions, based on 20 structures Valence Bond structures. The results are compared to CASSCF(4,4) calculations for both the energetics and the dipole moment. Additional calculations with partial electronic delocalization are presented, and it is shown that the dipole moment modification does not correspond to a situation where the antiaromatic situation prevails (with 4n electrons in the cycle). Part of the analysis uses a "trust factor" that helps to decide if a wave function is appropriate to describe a given state. The trust factor compares the VB wave function to the CASSCF's with their overlap. Finally, the Valence Bond density is used to produce density maps that illustrate the electron transfer upon excitation.

Keywords Valence Bond . Excited state. Electronic density . Dipole moment

Introduction

Methylenecyclopropene (MCP, Scheme 4) was first theoretically predicted to be stable (and with a strong dipole moment) back in the early 1950's[1][2][3]. But the first synthesis of the molecule was done more than 30 years after, in 1984, and the expected strong dipole moment was finally measured[4][5][6]. Substitution of the exocyclic position by more (or less) electronegative substituents give rise to very interesting effects[7][8]. The MCP molecule is also particularly interesting because of the inversion of the dipole moment upon excitation to the first singlet ($^1B_2$)[9]. A similar dipole inversion also occurs for the triplet[10][11]. Due to these dipole inversions, several studies have used MCP to discuss the environment's reorganization upon excitation[12]. Again, the molecule is sensitive to substitution and interesting effects are at work in the excited states of modified MCP, for instance in thio analogues[13].

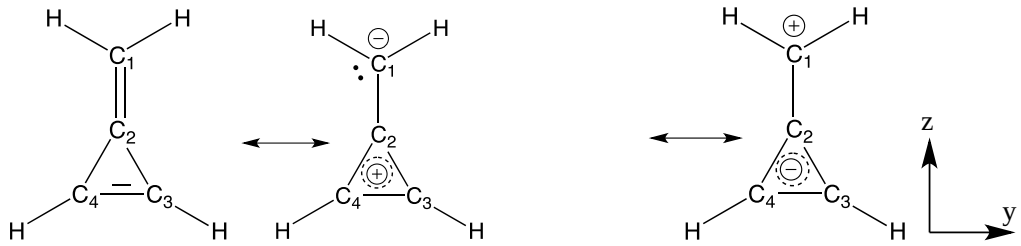

L₁ **L₂** **L₃**

Scheme 1: Usual Lewis structures for MCP with atoms numbering and orientation.

The MCP can be described by its *a priori* most important Lewis structure (**L₁**) as in Scheme 1. This structure **L₁** uses Bond Distorted Orbitals (BDO), extended on two atoms, to describe one π bond. The two other drawings are frequently used in the literature to express the charges associated to the dipole moment, **L₂** for the ground state with the normal dipole and **L₃** for the reverted dipole.

In this paper we use local wave functions (Valence Bond – like) to describe MCP in the ground state ($^1A_1$) and in its first excited state ($^1B_2$). Local wave functions are tested against a reference wave function such as the CASSCF(4,4) [14]. A trust factor (τ), which is simply the overlap with the reference wave function, is used for the test. Although CASSCF(4,4) is not the best wave function one can think about, it is well defined, and contains the main ingredients of these valence states. This will be discussed in the next section (computational details). Next, we will introduce the 20 structures of the Valence Bond calculations, and computed a few different localization constraints. Each time we used τ to discuss the reliability of the results for both the ground and the excited state. Finally density maps are presented and their meaning is linked to the electron shift upon excitation.

Computational level

Program, method and basis set

All calculations CASSCF calculations were carried out with GAMESS-US, version May 1 2013 (R1), [15] and we used the XMVB program to obtain the localized wave functions[16]. This program allows a total flexibility in the choice of the orbitals, with, for instance, no orthogonality constraint. In our calculations, the σ orbitals are common to all structures, but p_x orbitals are different from one structure to the other, which corresponds to the breathing orbitals formalism [17][18]. We used bi occupied CASSCF(4,4) optimized orbitals for the skeleton. The basis set is the 6-311+G(d) one[19][20]. We used the experimental geometry [21] reminded in the annex 2 below.

The results obtained with this level (CASSCF(4,4)/6-311+G(d)) are in reasonably good agreement with other computations. The vertical excitation energy for instance compares well with results of the literature VE=4.54 eV *vs* 4.81 eV for the SAC-CI[9], and around 4.20 eV for QMC computations (VMC-DMC) [12]. Similarly, the z-component of the dipole moment is well described, DMz=-1.78 D vs -1.99 D for the SAC-CI (see Table 1, entry 1). Additional computations that include the σ skeleton orbital relaxation through mono excitations of the σ electrons to σ* orbitals (RASSCF, entry 2) do not modify very significantly the results neither for the energy (VE=4.79 eV) nor for the dipole component (DMz=-1.90 D). The discrepancy with experimental values is usually attributed to the solvent and temperature effects as well as to the non-verticality of the experimental transition[22][23].

Comparison with the literature

The inversion of polarity between these two states [3] [4] [5] can be appraised with the modification of the sign of DMz. The value obtained with our CASSCF(4,4) computation of the $^1B_2$ excited state (+1.93 D, Table 1 entry 1) compares reasonably well with the literature. As a matter of fact it is more sensitive to the environment (solvent) than to the level of calculation. Again, the RASSCF calculation on the $^1B_2$ excited state wave function, entry 2, does not modify significantly the results (DMz=+1.80 D).

Table 1. Vertical excitation energies (VE) from 1 $^1A_1$ state to 1 $^1B_2$ state: $VE=E_{ES}-E_{GS}$ (eV), and z-component of the dipole moment (DMz) in each state. Unless explicitly stated, values are obtained in vacuum.[b,c]

	VE	DMz (1 $^1A_1$)	DMz (1 $^1B_2$)
CAS(4,4)[a]	4.54	-1.78	+1.93
RASSCF[a]	4.79	-1.90	+1.80
CAS(4,4) [d]	4.56	-1.79	+1.92
HF/CIS[9]	5.51	-2.39	+2.60

SAC/SAC-CI[9]	4.81	-1.99	+2.34
SAC-CI vacuum[24]	4.76	-1.86	+1.19
SAC-CI-water[24]	4.87	-2.46	+1.42
SAC-CI-n-hexane[24]	4.70	-	-
CAS(4,5) [22]	4.71	-1.80	+2.07
CASPT2 [12][22]	4.13	-	-
VMC-DMC-vacuum [12]	4.14 – 4.26	-	-
VMC-DMC-water [12]	4.83 – 5.01	-	-
Exp[b] [4]	4.49	-	-
Exp[c] [4]	4.01	-1.90	-

[a] This work, 6-311+G(d) basis set. [b] In methanol -78 °C. [c] In n-pentane -78 °C. [d] from [23] the cc-pVTZ basis set was used.

Choice of VB structures

Twenty-one Valence Bond structures, which use only atom-centered orbitals, are obtained by the distribution of the four π electrons on the four carbon centers. As shown in scheme 2, they are neutral (labeled $\mathbf{n_1}$, $\mathbf{n_2}$, …), ionics (labeled $\mathbf{i_1}$, $\mathbf{i_2}$, …), and di-ionics (labeled $\mathbf{d_1}$, $\mathbf{d_2}$, …). Removing one of the three neutral structures circumvents a hidden redundancy between them. We removed $\mathbf{n_1}$ in order to have the possibility to deal with wave functions that are either symmetrical or anti symmetrical toward the σ_{xz} plan of symmetry (in the C_{2v} point group).

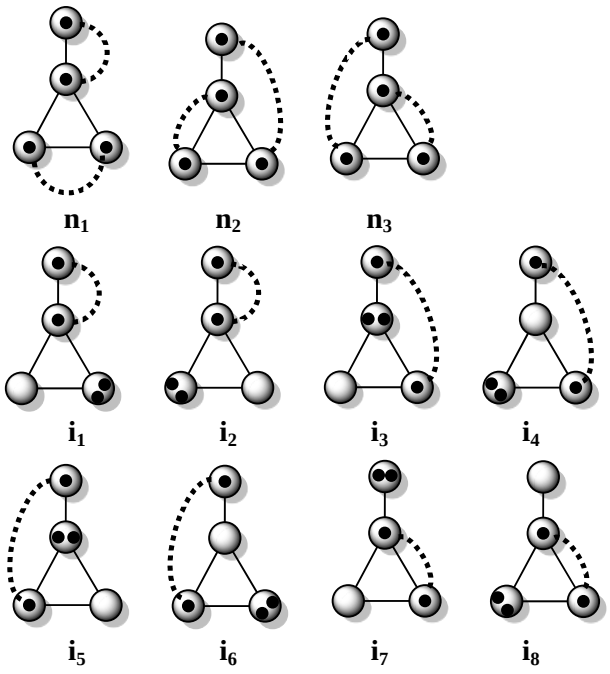

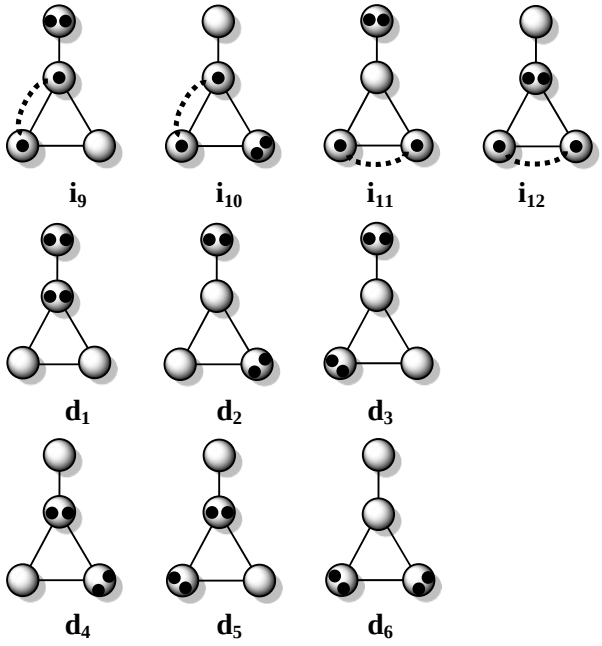

Scheme 2: Valence Bond structures. Each circle represents a p_x atom-centered orbital. A bi occupied orbital corresponds to a negative charge and an empty one to a positive charge. Dashed lines represent singlet coupling between two electrons on two different centers.

Results and discussion

Energies of the structures

In a first stage, the p_x orbitals were pre-optimized for the ground state of each individual structure. The relative energies of the structures are displayed in Table 2. They are relative to $\mathbf{n_1}$. Not surprisingly, neutral structures are lower than ionics and di ionics. Among the energies displayed in Table 2 one ionic structure ($\mathbf{i_{11}}$) is particularly low in energy compared to others. This structure $\mathbf{i_{11}}$ clearly fulfills the Hückel rule for aromaticity: it has 4n+2 π electrons in the 3-membered cycle.[25, 26] The same seems to happen when comparing the energies of structures $\mathbf{i_7}$ (9.27 eV), which has two electrons in the cycle, to $\mathbf{i_8}$ (13.88 eV), which has four electrons. Similarly, the di ionic structures $\mathbf{d_2}$ and $\mathbf{d_3}$ are particularly low in energy compared to other di ionic structures. It corresponds again to structures with 4n+2 electrons in the cycle. However, repulsions between neighboring charges of same sign have a large effect on the energetics. Structure $\mathbf{d_1}$ and $\mathbf{d_6}$ for instance have two neighboring positive charges and two neighboring negative charges. They are higher in energy than $\mathbf{d_4}$ and $\mathbf{d_5}$, which have only repulsion between negative charges.

Table 2. Relative energy of independently optimized VB structure (eV) with frozen σ orbitals from the CAS(4,4) ground state calculation.

HF	-1.77
CAS(4,4)	-3.03
$\mathbf{n_1}$	0.00
$\mathbf{n_2}$[a]	3.69
$\mathbf{i_1}$[a]	6.39
$\mathbf{i_3}$[a]	9.49
$\mathbf{i_4}$[a]	10.24
$\mathbf{i_7}$[a]	9.27
$\mathbf{i_8}$[a]	13.88
$\mathbf{i_{11}}$	4.81
$\mathbf{i_{12}}$	8.39
$\mathbf{d_1}$	20.29
$\mathbf{d_2}$[a]	11.76
$\mathbf{d_4}$[a]	14.23
$\mathbf{d_6}$	25.77
[a] due to symmetry, $E_{n3}=E_{n2}$, $E_{i2}=E_{i1}$, $E_{i5}=E_{i3}$, $E_{i6}E_{i4}$, $E_{i9}=E_{i7}$, $E_{i10}=E_{i8}$, $E_{d3}=E_{d2}$, $E_{d5}=E_{d4}$.	

Trust factor

The VB wave function for the ground state can be approximated using pre optimized p_x orbitals. In any case we will compare the VB computations to the CASSCF, both for the energetics and for the wave function. To compare the wave functions, we recently used their overlap as a guide [14]. The overlap between a reference wave function and the VB wave function is called the "trust factor" and is labeled τ[14] [27].When τ = 100% the agreement between the CASSCF and the VB wave function is perfect. Hence, they describe the same state with the same wave function. A value τ= 0% indicates that the VB wave function describes another state. The trust factor is particularly interesting when the wave function is defined on the basis of numerous Slater determinants.

Ground state results $1\ ^1\mathbf{A_1}$

As shown in Table 3 at step 0, when the orbitals are optimized on the independent VB structures, the trust factor is already satisfactory (97.2%), and the orbitals optimization gives a rather small improvement (99.5%).

However, the energy of the ground state is lowered by about 1.40 eV when the orbitals are optimized so the small improvement of τ correspond to a significant effect on the energetics. As shown in equation 1 (see also annex 2), the ground state in mainly represented by the combination of (c_2+c_3), i_{11} and (i_1+i_2). The in-phase combination between c_2 and c_3 is consistent with the A_1 symmetry of this state. The prominent coefficient of i_{11} in the wave function is the key of the charge separation in the Ground State. When Coulson-Chirgwin [28][29] weights are computed (Figure 1), i_{11} has a weight of about 15%, which is almost as large as that of a covalent structure (c_2 or c_3), 22%. Last note that twelve structures contribute to the ground state with very low weights, but their total cumulated weight is significant 13%. This corresponds to a large delocalization, where many structures must be defined to obtain a reasonable description. This tendency is magnified in benzene where 175 VB structures must be used [30].

Table 3. Absolute and relative energy for HF, CAS and optimized VB wave function (eV). The relative energies are relative to the CASSCF calculation on the ground state.

		τ (%)/CASSCF	E (Hartree)	DE (eV)
VB 1 $^1A_1$	iter=0	97.2	-153.69477	1.40
	π Opt	99.5	-153.74351	0.07
VB 1 $^1B_2$	iter=0	93.2	-153.50937	6.45
	π Opt	96.5	-153.55200	5.29
CAS(4,4) 1 $^1A_1$	-	-	-153.74626	0.00
CAS(4,4) 1 $^1B_2$	-	-	-153.57928	4.54

$$\Psi^{VB}(^1A_1)=0.44\ (c_2+c_3) - 0.22\ i_{11} - 0.13\ (i_1+i_2) + \ldots \quad (1)$$

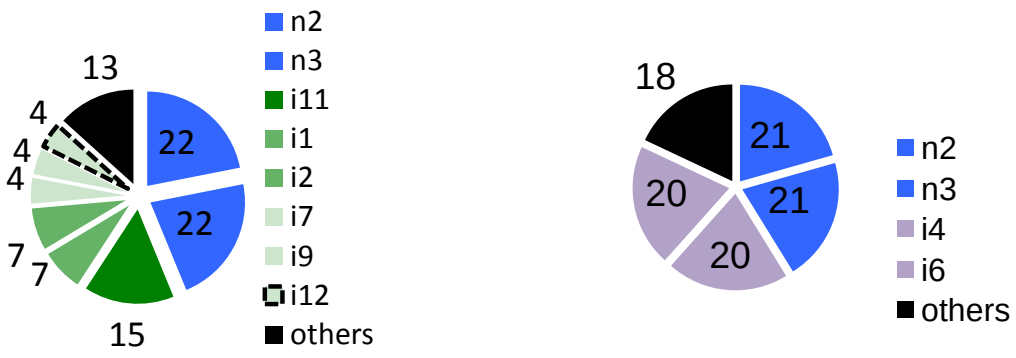

Figure 1: Weights (%) of the VB structures of MCP. (a) left, for the 1 $^1A_1$ ground state; The black

sector called "other" is a summation of the weights of all other (12) VB structures. (b) right, for the 1 $^1B_2$ first singlet excited state. The black sector corresponds to 16 structures.

Excited state-1 $^1B_2$

Similar results are obtained for the first singlet excited state. A small improvement of the trust factor is obtained upon π orbitals optimization. The energy is lowered by about 1.2 eV. The expression of this state in the basis of the VB structures is displayed in equation 2 (see also annex 2). The out-of-phase combination between the neutral structures is consistent with the B_2 symmetry.

$$\Psi^{VB}(^1B_2)=0.32\ (n_2–n_3) + 0.30\ (i_4–i_6)\ i_{11} + 0.16\ (i_1–i_2) + \ldots \quad (2)$$

Choice of the σ orbitals (using pre optimized π orbitals)

For the calculation on the excited state we used the σ orbitals of the $^1B_2$ state from the CASSCF calculation. One shall wonder how important are these σ orbitals. Replacing them by the orbitals of the ground state rises the energy by 0.5 eV: it is situated at 6.95 eV above the ground state CASSCF energy, instead of 6.45 eV when more appropriate σ orbitals from the CASSCF ground state calculation are used. The trust factor is also only slightly modified (92.2% instead of 93.2%). The polarization of the state can be seen with the DMz value: when ground state σ orbitals are used for the excited state DMz=+2.35 D. When more appropriate σ orbitals from the CASSCF calculation of the excited state are used, DMz=+2.04 D. The reversed dipole is always correctly obtained. These values contrast with the ground state value of -1.81 D when the Valence Bond wave function is computed for the ground state (with ground state orbitals for the σ orbitals). Hence, the dipole is not very sensitive to the choice of the σ orbitals.

π orbitals optimization

Finally, the π orbitals optimization is of much larger importance for the energy than for the dipole moment orientation or for the trust factor. Table 4 reports the DMz values obtained for each state when σ orbitals from the appropriate CASSCF calculation are used and π orbitals are optimized. The values are in the same range. The corresponding effective charge on carbon 1 is also given. To obtain this value, we defined the dipole on the carbon 1 and on the center of mass of the carbons of the 3-membered ring [31]. These two points are distant by d=2.185 Å. We observed the inversion of polarity on the charges.

Table 4. Dipole moment on z-axis DMz (Debye) and corresponding effective charge on carbon 1[a] Q_1^{eff} of triafulvene.

State	$1\ ^1A_1$	$1\ ^1B_2$
DMz	-2.12	2.00
Q_1^{eff}	-0.20	0.19
[a] For calculation of effective charge, the distance used (in $\mu = Q_1^{eff}$ d) is d=2.185 Å. See text.		

Link with Lewis structures

The computations done with the Valence Bond formalism can be more compact if delocalized Lewis structures are used for the wave function (**L_1**, **L_2**, **L_3**, Scheme 1). They correspond to standard drawings for this system. In order to avoid a strong polarization of the orbital describing the exocyclic π bond in **L_1**, and some related redundancy between **L_1** and **L_2**, we used **n_1** and **L_2** instead of **L_1** and **L_2**. The way to obtain the delocalized Lewis structures **L_2** and **L_3** is to allow a partial electronic delocalization over the three carbon atoms of the cycle, while keeping the charge on the exo cyclic atom in a strictly localized orbital ($2b_1$, Figure 2). For **L_2**, the configuration is $(1b_1)^2(2b_1)^2$. This structure is of A_1 symmetry. There are three ways to obtain **L_3**. One is to consider a mixture of doubly occupied orbitals $(1b_1)^2(3b_1)^2$ and $(1b_1)^2(a_2)^2$. This gives two **L_3** structures of A_1 symmetry (**$L_{3'}$** and **$L_{3''}$**). In our computation, **$L_{3'}$** and **$L_{3''}$** share the same $1b_1$ orbital, and are pre optimized together. The other way to obtain **L_3** is to consider the open shell singlet structure $(1b_1)^2(3b_1)^1(a_2)^1$, which is of B_2 symmetry. This open shell structure is labeled **$L3_{os}$** in the following. **L_{3os}** can only describe the $^1B_2$ excited state. However, a contrario to the orbitals of **$L_{3'}$** and **$L_{3''}$** which smoothly optimized, it was not possible to optimize the orbitals of **L_{3os}** at the singlet state without severe rotations between the three active orbitals. Hence, because the orbitals involved in the open shell singlet or in the triplet are probably alike, we optimize them for the triplet, and use them "as is" for the open shell singlet, **L_{3os}**, without any additional optimization.

For the ground state, the Coulson-Chirgwin weights of the four structures calculation (**n_1**, **L_2**, **$L_{3'}$**, **$L_{3''}$**) are 59.9, 30.5, 9.7 and 0.1% with pre-optimized orbitals. These weights are similar if the π orbitals are optimized for the ground state (56.8, 31.3, 11.6 and 0.2 %). When this is the case, the energy is lowered by 0.45 eV, and the trust factor is as large as τ=98.4% (Table 5). It is nice to see that the large weight of **L_2** is consistent with the dipole moment. Moreover, structure **L_2** has a strong aromatic character (it contains 4n+2 = 6 π electrons), and its important role in the ground state is consistent with standard rules of aromaticity. The value we obtain here for **L_2** is somehow larger than that found by Radom based on a two structures calculation, with only Mulliken charges (19%) [31].

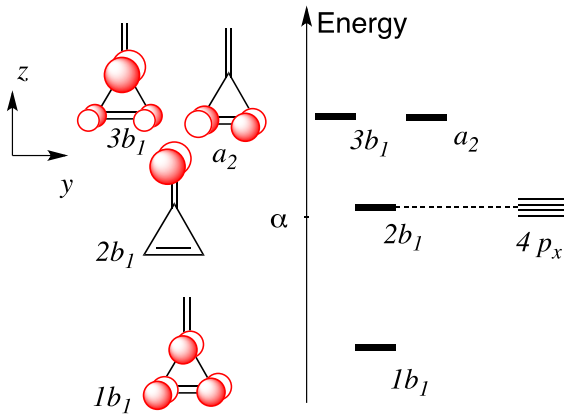

Figure 2: Partial electronic delocalization, C_{2v} labels of the orbitals, Hückel-like drawings.[32]

It would be nice to describe the excited state on the basis of these 3 structures: due to the dipole inversion one would predict $\mathbf{L_3}$ to have a prominent role in the wave function of the excited state. It has also some anti aromatic character, and this would fit with an extension of Baird's rule from the triplet to specific singlets [33]. However, the $^1B_2$ state is very poorly described with such a description. Using the aforementioned guess orbitals for $\mathbf{L_{3os}}$ we obtained a trust factor of only 51.9%, which is extremely low. Moreover, the mean value of the energy (13.2eV) is not even in the range of the targeted state. The 20 VB structures calculation gives a much more accurate description and this description should be used. The large weights of $\mathbf{i_4}$ and $\mathbf{i_6}$ correspond to a state that has some bi radical components involving C1. In $\mathbf{L_{3os}}$ the exo cyclic atom is not part of the singlet coupling, which explains that this structure is not relevant. However, using the same orbitals, another configuration can be defined: $\mathbf{L_{3os}'''}=(1b_1)^2\ (2b_1)^1\ (a_2)^1$. It also describes a singlet coupling of B_2 symmetry, but involves the exocyclic carbon.

With this $\mathbf{L_{3os}'''}$ structure, the π orbital optimization was smooth, and the state we obtained overlaps with the CASSCF calculation with a trust factor of τ = 96.5 %, which shows that the appropriate state was obtained. Moreover, the mean value of the energy is in the range of the energy of the state, 5.73 eV. The z-component of the dipole moment is compatible with a positive charge on the C1 atom (DMz=+1.48 D) although the structure does not have an explicit positive charge on the C1 atom. Last, we shall note that the energy error made on the ground state is of the same magnitude as that of the excited state. The error compensation leads to an energy difference between the ground and excited state of 5.04 eV, in reasonable agreement with other computations. For instance CASSCF gives 4.54 eV, and the 20 structures VB gives 5.21 eV.

Table 5: Calculations based on delocalized Lewis structures

	τ (%)/CASSCF	E (Hartree)	eV

LEWIS 1 $^1A_1$	iter=0	93.2	-153.70446	1.14
$\mathbf{L_1}$, $\mathbf{L_2}$, $\mathbf{L_{3'}}$$\mathbf{L_{3''}}$	Opt	98.4	-153.72092	0.69
LEWIS 1 $^1B_2$	iter=0	51.9[a]	-153.26162[a]	13.2[a]
$\mathbf{L_{3os}}$[a]	Opt	-	-	-
$\mathbf{L_{3os'''}}$	Iter=0	96.5	-153.53558	5.73
CAS(4,4) 1 $^1A_1$	/	/	-153.74626	0.00
CAS(4,4) 1 $^1B_2$	/	/	-153.57928	4.54

[a] Due to orbital rotations in the singlet B_2 state, active orbitals $1b_1$, $3b_1$, a_2 for $\mathbf{L_{3os}}$ were optimized for the triplet B_2 instead.

Density analysis

In the following we use the electronic density difference between the ground and the excited states ($\rho(^1B_2)$-$\rho(^1A_1)$). This difference is plotted in figure 3 with green color for positive density difference, and red for negative. The drawing was made from the Valence Bond wave functions based on the 20 VB structures, although a similar picture can be obtained at the CASSCF level. The figure shows the charge transfer upon excitation.

Figure 3: Top view (left) and side view of the electronic density difference map of MCP between the excited state $^1B_2$ and the ground state $^1A_1$. An isovalue of + and – 1.10^{-2} a.u. was used. Red contours correspond to areas where the electron density is smaller in the excited state than in the ground state.

From the ground state to excited state, carbons 1 and 2 lost some π electronic density (red). The π bond between carbon 3 and 4 also lost some electronic density (red), but the atomic π density increased on theses carbons. This map correlates well with the discussion on the Lewis structures and with the importance of the ionic structures $\mathbf{i_4}$ and $\mathbf{i_6}$ in the excited state.

The isodensity contours can be nicely completed by the computation of actual electron displacement if we integrate the density difference in volumes [34]. The algorithm developed by Tognetti et al integrates the density when it is larger (respectively smaller) than a threshold. With a threshold of +0.01, we obtained a unique volume where 0.70 electrons are gained upon excitation. It is shown as green dots on Figure 4. If we request a similar volume calculation of negative density difference, two

volumes are obtained. They are displayed as red dots. Finally, upon excitation, more than half an electron quits the exocyclic π bond and locates itself on the C3 and C4 atoms of the cycle.

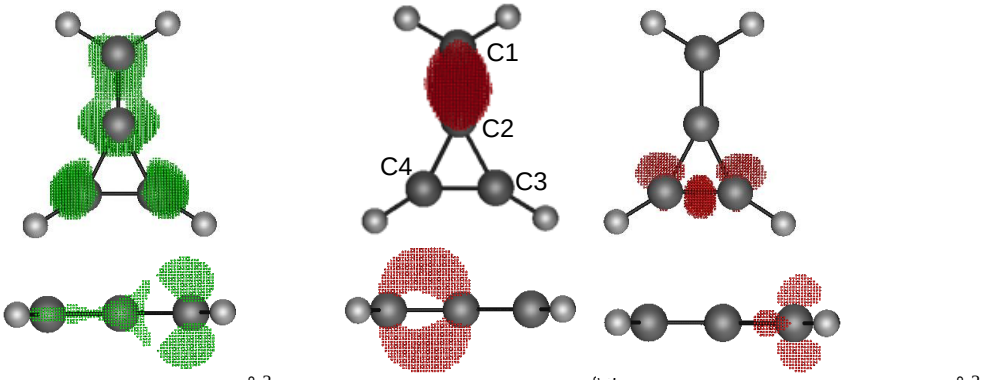

Figure 4: Density integrated on positive/negative values.

Conclusions

Triafulvene, its strong dipole, and its dipole inversion upon excitation were studied with rather simple VB computations. Our study might appear somehow narrow on the multi-determinantal reference computations (CASSCF(4,4)) which contains only 18 determinants. However, we showed that going to the RASSCF level (3330 determinants) would not change significantly the qualitative description of the states at work: the dipoles are roughly alike, and the dipole inversion is also similar. The Valence Bond description showed that the nature of the two states could be understood with a small number of structures. In order to orient our study in the direction of usual Lewis structures writings, we used partially delocalized orbitals. We have chosen the orbitals in such a way that two parts were considered: the three-membered ring part and the exocyclic part. This partition corresponds to the known electronic displacement that occurs in the ground state and upon excitation. We showed that among the possible orbital configurations, one was particularly relevant for the $^1B_2$ state ($\mathbf{L}_{3os'''}$). This single structure overlaps at 96.5% with the CASSCF(4,4) wave function, and the dipole moments are consistent: we obtained DMz=+1.48 D for $\mathbf{L}_{3os'''}$ alone *vs* +1.93 for the CASSCF(4,4)). Despite the fact that the structure $\mathbf{L}_{3os'''}$ has the correct dipole orientation, it does not display the expected positive net charges on the exo cyclic C1 atom: the $2b_1$ orbital (Figure 2) is filled with a single electron, hence the exo cyclic carbon has no net charge.

Differences of densities between the two states were used to illustrate the charge modification at work upon excitation. This analysis showed an electronic modification of the π electrons from the C1-C2 part of the molecule toward the C3-C4 carbon atoms of the cycle. A small repolarisation of the σ electron can also be observed.

Acknowledgments

Professor Wei Wu at Xiamen University is gratefully acknowledged for the XMVB code. The authors acknowledge also Dr. Tognetti and Pr. Christophe Morell for the access to the Descriptor algorithm to integrate the density differences.

Keywords: valence bond, excited states, electronic density.

Annexes

Annex 1: Geometry

Experimental C_{2v} geometry* has been used for all calculation of the methylenecyclopropene [21].

C1	0.00000	0.00000	0.00000
C2	0.00000	0.00000	-1.33200
C3	0.00000	0.66203	-2.61192
C4	0.00000	-0.66203	-2.61192
H5	0.00000	0.93003	0.55882
H6	0.00000	-0.93003	0.55882
H7	0.00000	1.57289	-3.19220
H8	0.00000	-1.57289	-3.19220

- xyz coordinates are given in angstroms

Annex 2: Coefficients obtained in the Valence Bond computation (20 structures)

	1 $^1A_1$	**1 $^1B_2$**
n_2	-0.444987	-0.323074
n_3	-0.444996	0.323145
i_1	0.132939	0.160384
i_2	0.132919	-0.160388
i_3	-0.081109	-0.065502
i_4	0.025782	-0.298112
i_5	-0.081106	0.065508
i_6	0.025796	0.298015
i_7	0.122252	0.023539

i_8	0.014324	-0.118728
i_9	0.122253	-0.023525
i_{10}	0.0143050	0.118755
i_{11}	0.2227071	-0.000018
i_{12}	0.0968362	-0.000011
d_1	-0.013665	-0.000005
d_2	0.072615	0.060520
d_3	0.072644	-0.060652
d_4	0.020758	0.035776
d_5	0.020756	-0.035781
d_6	-0.006709	-0.000105

References and Notes

1. Berthier G, Pullman B (1949) Configuration géométrique et moment dipolaire des hydrocarbures conjugués. Bull Soc Chim Fr 16:D457–D465.

2. Syrkin Y, Dyotkina M (1946) The resonance Energies of the polynuclear hydrocarbon. Bull Académie Sci URSS 2:153–178.

3. Roberts JD, Streitwieser Jr A, Regan CM (1952) Small-Ring Compounds. X. Molecular Orbital Calculations of Properties of Some Small-Ring Hydrocarbons and Free Radicals1. J Am Chem Soc 74:4579–4582.

4. Staley SW, Norden TD (1984) Synthesis and direct observation of methylenecyclopropane. J Am Chem Soc 106:3699–3700.

5. Billups WE, Lin LJ, Casserly EW (1984) Synthesis of methylenecyclopropene. J Am Chem Soc 106:3698–3699.

6. Maier G, Hoppe M, Lanz K, Reisenauer HP (1984) Neue wege zum cyclobutadien und methylencyclopropen. Tetrahedron Lett 25:5645–5648.

7. Saebø S, Stroble S, Collier W, et al. (1999) Aromatic Character of Tria- and Pentafulvene and Their Exocyclic Si, Ge, and Sn Derivatives. An ab initio Study. J Org Chem 64:1311–1318.

8. Najafian K, von Ragué Schleyer P, Tidwell TT (2003) Aromaticity and antiaromaticity in fulvenes, ketocyclopolyenes, fulvenones, and diazocyclopolyenes. Org Biomol Chem 1:3410–3417.

9. Nakajima T, Nakatsuji H (1999) Energy gradient method for the ground, excited, ionized, and electron-attached states calculated by the SAC (symmetry-adapted cluster)/SAC–CI (configuration interaction) method. Chem Phys 242:177–193.

10. Möllerstedt H, Piqueras MC, Crespo R, Ottosson H (2004) Fulvenes, Fulvalenes, and Azulene: Are They Aromatic Chameleons? J Am Chem Soc 126:13938–13939.

11. Rosenberg M, Dahlstrand C, Kilså K, Ottosson H (2014) Excited State Aromaticity and Antiaromaticity: Opportunities for Photophysical and Photochemical Rationalizations. Chem Rev 114:5379–5425.

12. Guareschi R, Zulfikri H, Daday C, et al. (2016) Introducing QMC/MMpol: Quantum Monte Carlo in Polarizable Force Fields for Excited States. J Chem Theory Comput 12:1674–1683.

13. Serrano-Andrés L, Pou-Amérigo R, Fülscher MP, Borin AC (2002) Electronic excited states of conjugated cyclic ketones and thioketones: A theoretical study. J Chem Phys 117:1649.

14. Racine J, Hagebaum-Reignier D, Carissan Y, Humbel S (2016) Recasting wave functions into valence bond structures: A simple projection method to describe excited states. J Comput Chem 37:771–779.

15. Schmidt MW, Baldridge KK, Boatz JA, et al. (1993) General atomic and molecular electronic structure system. J Comput Chem 14:1347–1363.

16. Chen Z, Ying F, Chen X, et al. (2015) XMVB 2.0: A new version of Xiamen valence bond program. Int J Quantum Chem 115:731–737.

17. Hiberty PC, Humbel S, Byrman CP, Lenthe JH van (1994) Compact valence bond functions with breathing orbitals: Application to the bond dissociation energies of F2 and FH. J Chem Phys 101:5969–5976.

18. Hiberty PC, Shaik SS (2002) Breathing-orbital valence bond method—a modern valence bond method that includes dynamic correlation. Theor Chim Acta 108:255–272.

19. Clark T, Chandrasekhar J, Spitznagel GW, Schleyer PVR (1983) Efficient diffuse function-augmented basis sets for anion calculations. III. The 3-21+G basis set for first-row elements, Li-F. J Comput Chem 4:294–301.

20. Krishnan R, Binkley JS, Seeger R, Pople JA (1980) Self-consistent molecular orbital methods. XX. A basis set for correlated wave functions. J Chem Phys 72:650–654.

21. Norden TD, Staley SW, Taylor WH, Harmony MD (1986) Electronic character of

methylenecyclopropene: microwave spectrum, structure, and dipole moment. J Am Chem Soc 108:7912–7918.

22. Merchant M, González-Luque R, Roos BO (1996) A theoretical determination of the electronic spectrum of Methylenecyclopropene. Theor Chim Acta 94:143–154.

23. Cammi R, Frediani L, Mennucci B, et al. (2002) A second-order, quadratically convergent multiconfigurational self-consistent field polarizable continuum model for equilibrium and nonequilibrium solvation. J Chem Phys 117:13–26.

24. Cammi R, Fukuda R, Ehara M, Nakatsuji H (2010) Symmetry-adapted cluster and symmetry-adapted cluster-configuration interaction method in the polarizable continuum model: Theory of the solvent effect on the electronic excitation of molecules in solution. J Chem Phys 133:024104.

25. Solà M (2013) Forty years of Clar's aromatic π-sextet rule. Front Chem. doi: 10.3389/fchem.2013.00022

26. Khatmi D, Carissan Y, Hagebaum-Reignier D, et al. (2016) Mesomerism, Ring & Substituent Effects, A Computational Chemistry Experiments. J Lab Chem Educ 4:25–34.

27. Carissan Y, Hagebaum-Reignier D, Goudard N, Humbel S (2008) Hückel-Lewis Projection Method: A "Weights Watcher" for Mesomeric Structures. J Phys Chem A 112:13256–13262.

28. Chirgwin BH, Coulson CA (1950) The Electronic Structure of Conjugated Systems. VI. Proc R Soc Lond Math Phys Eng Sci 201:196–209.

29. Thorsteinsson T, Cooper DL (1998) Nonorthogonal weights of modern VB wave functions. Implementation and applications within CASVB. J Math Chem 23:105–126.

30. Norbeck JM, Gallup GA (1974) Valence-bond calculation of the electronic structure of benzene. J Am Chem Soc 96:3386–3393.

31. Scott AP, Agranat I, Biedermann PU, et al. (1997) Fulvalenes, Fulvenes, and Related Molecules: An ab Initio Study. J Org Chem 62:2026–2038.

32. Carissan Y, Goudard N, Hagebaum-Reignier D, Humbel S (2016) Localized Structures at the Hückel Level, a Hückel-Derived Valence Bond Method. In: Appl. Topol. Methods Mol. Chem., Springer International Publishing. Chauvin, R., Lepetit, C., Silvi, B., Alikhani, E., Cham, pp 337–360

33. Baird NC (1972) Quantum organic photochemistry. II. Resonance and aromaticity in the lowest 3. pi.. pi.* state of cyclic hydrocarbons. J Am Chem Soc 94:4941–4948.

34. Tognetti V, Morell C, Joubert L (2015) Quantifying electro/nucleophilicity by partitioning the

dual descriptor. J Comput Chem 36:649–659.